Ultrasonics 138 (2024) 107236

Contents lists available at ScienceDirect

Ultrasonics

journal homepage: www.elsevier.com/locate/ultras

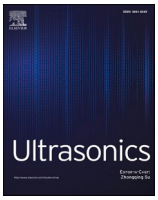

Ultrasonic fatigue of unfilled and carbon nanotube (CNT) reinforced polyetheretherketone (PEEK)

Michael Fitzka [a], Bernd M. Schönbauer [a], Viktor Stojanovic [a], Harald Rennhofer [a], Helga Lichtenegger [a], Jason W. Carroll [b], Niloofar Sanaei [b], Javed Mapkar [b], Herwig Mayer [a,*]

[a] Institute of Physics and Materials Science, University of Natural Resources and Life Sciences (BOKU) Vienna, 1190 Vienna, Austria
[b] Center for Materials and Manufacturing, Eaton Corporation, Southfield, MI 48076, United States of America

ARTICLE INFO

Keywords:
Very high cycle fatigue
Plastic
Reinforced polymer
Strain rate effect
Fatigue limit

ABSTRACT

Fatigue properties of polyetheretherketone (PEEK) and multiwall carbon nanotube (CNT) reinforced PEEK were investigated with the ultrasonic fatigue testing method. Lifetimes were measured in the high and very high cycle fatigue regime at resonance frequency 19 kHz and load ratio R = -1. Pulse-pause loading served to avoid specimen self-heating and led to effective cycling frequencies in the range from several hundred Hz to about two kHz. Stress amplitude for 50 % fracture probability at 10^9 cycles is 21.2 ± 4.3 MPa for unreinforced PEEK (22 % of its tensile strength) and 33.5 ± 3.5 MPa for CNT reinforced PEEK (33 % of its tensile strength). Servohydraulic fatigue tests at 22 Hz with CNT reinforced PEEK delivered fatigue lifetimes comparable to ultrasonic tests, i.e. no frequency effect and no influence of load versus displacement control was observed. Keeping specimen temperature far below the glass transition temperature, ultrasonic fatigue testing of a high temperature resistant plastic was successfully implemented.

1. Introduction

Ultrasonic fatigue testing is a method ideally suited to investigate the high cycle fatigue (HCF) and very high cycle fatigue (VHCF) properties of materials [1]. Cycling specimens in resonance at about 20 kHz strongly reduces testing times compared with servohydraulic, rotating bending or reversed bending tests with typical test frequencies below 100 Hz. Ultrasonic fatigue testing is well established for testing metallic materials [2,3], whereas investigations of (reinforced) polymers are limited. One reason is the concern about excessive self-heating under high frequency vibration, and potential cooling problems due to the low thermal conductivity coefficient of plastics (~0.2 – 0.5 W/m/K) compared to metals (~20 – 300 W/m/K). A possible frequency influence on the measured fatigue data is another reason for the limited number of ultrasonic investigations on unfilled and reinforced plastics.

A strong increase of specimen temperature during continuous cycling at ultrasonic frequency is reported for acrylonitrile butadiene styrene (ABS) [4] and polymethylmethacrylate (PMMA) [5], although the specimens were tested submerged in liquids for good cooling. A technique to limit self-heating of specimens in ultrasonic tests is to perform the experiments in pulsed mode with intermittent cooling pauses. Axial loading ultrasonic fatigue tests in pulsed mode have been performed with glass fiber reinforced polymer (GFRP) [6,7]. Cyclic tension tests at load ratio $R = 0.1$ have been conducted up to the VHCF regime (i.e. above 10^7 cycles) with ultrasonic equipment and up to the HCF regime with servohydraulic equipment, and similar fatigue lifetimes were found for 20 kHz and 10 Hz in the overlapping regime of *S-N* data [6]. Lower fatigue lifetimes at 20 kHz compared to 3 Hz were found in cyclic tension compression tests (R = -1) of GFRP [7]. The differing findings concerning frequency effects in GFRP can be explained considering specimen temperature during high frequency loading and glass transition temperature of the polymer matrices [8]: Specimen temperatures were close to the glass transition temperature in the investigation showing a frequency effect [7] and significantly below in the other investigation [6]. Ultrasonic tension–compression fatigue tests have been performed with carbon fiber reinforced polymer (CFRP) produced as quasi-isotropic laminate, and no endurance limit below 10^9 cycles was found [8]. The effect of fiber orientation with respect to the loading direction was studied in ultrasonic tests of CFRP produced with 3D printing technology [9]. Both investigations were performed in pulsed mode with effective frequencies up to 2 kHz [8], and 600 Hz [9]. This is significantly higher than cycling frequencies used in servo-

* Corresponding author.
E-mail address: herwig.mayer@boku.ac.at (H. Mayer).

https://doi.org/10.1016/j.ultras.2023.107236
Received 18 September 2023; Received in revised form 24 November 2023; Accepted 27 December 2023
Available online 30 December 2023

hydraulic VHCF tests of CFRP, where test frequencies of 158 Hz [10] and at 100 Hz [11] are reported. Axial loading ultrasonic fatigue tests with aramid fiber reinforced aluminum laminates (ARALL) demonstrated the strong beneficial effect of bridging fibers behind the crack tip on slow fatigue crack growth and threshold stress intensity [12]. Similar tests with glass fiber reinforced aluminum laminates (GLARE) with different blunt notches additionally showed beneficial effects of fibers on crack initiation and initial crack growth [13].

A three point bending ultrasonic fatigue testing method has been newly developed and used to investigate the VHCF properties of carbon fiber reinforced polymers (CFRP) [14]. The progress of fatigue damage in CFRP could be identified with this method for different ranges of VHCF lifetimes [15,16]. Ultrasonic cyclic bending tests served to demonstrate the beneficial effect of incorporating nano-silica [17] and multiwall carbon nanotubes [18] into the matrix of CFRP, as well as for studies of the influence of temperature and humidity [19] and UV radiation [20] on cyclic strength. Axial loading ultrasonic fatigue tests of CFRP at $R = -1$ are also reported in the literature [21,22], and cyclic strength comparable to servohydraulic tests is found [22]. Stress and strain calculations as well as vibrometer measurements for CFRP subjected to axial and bending loading are available in [23].

Besides technical materials, the fatigue properties of wood as a natural fiber reinforced polymer (i.e. cellulose fibers embedded in a lignin matrix) have been studied with ultrasonic fatigue testing. Sycamore maple [24] and birch wood [25] have been subjected to cyclic tension–compression loading with ultrasonic equipment at 20 kHz, and with servohydraulic equipment at 50 Hz. Similar fatigue lifetimes in the HCF regime were found for both wood species cycled at both frequencies indicating no strain rate effect for wood. Ultrasonic tests were performed up to the VHCF regime showing no fatigue limit in wood below 10^9 cycles [24,25].

In the present investigation, ultrasonic fatigue tests are performed in the HCF and VHCF regime with polyetheretherketone (PEEK) and with multiwall carbon nanotube (CNT) reinforced PEEK. Additional servohydraulic tests are performed in the HCF regime. PEEK is a thermoplastic polymer with excellent mechanical properties at room and elevated temperatures, which can be further enhanced by reinforcement with fibers or particles. It is widely used in automotive and aerospace industry (e.g. for bearings, piston parts, pumps, and compressor plate valves), and selected grades are utilized for dentistry or long-term orthopedic implants. The material is subjected to cyclic stresses in these applications, and fatigue properties need to be known therefore. In particular, reliable fatigue data are necessary up to the VHCF regime since engine components and medical implants may be loaded with several hundred million cycles during service.

Several investigations about the fatigue properties of PEEK are available in the literature. Fatigue crack growth studies [26], and fatigue lifetime measurements in presence of different notches [27], under multiaxial loading [28], for different mean loads [29,30] and at different cycling frequencies [29,31] are reported. It is demonstrated that reinforcement with short glass [32] or carbon fibers [33,34] improves the fatigue crack growth properties, and short carbon fibers increase the cyclic load necessary for crack nucleation [35]. Investigations on the fatigue properties of unfilled and reinforced PEEK are, however, currently limited to the HCF regime.

The present investigation demonstrates the application of the ultrasonic fatigue testing technique to acquire HCF and VHCF lifetimes of PEEK and CNT reinforced PEEK. Due to the relatively low stiffness and high strength values of the materials, large strain amplitudes and consequently high displacement amplitudes must be applied and accurately controlled. Specimens are designed to generate sufficiently high strain amplitudes within the operational limits of the ultrasonic system. Accurate control of displacement amplitudes is verified with optical methods in conjunction with finite element analysis (FEA). Fatigue tests are performed at $R = -1$ with ultrasonic equipment. Comparative tests with servohydraulic equipment in an overlapping regime of fatigue lifetimes serve to validate ultrasonic data and to identify possible influences of test method and cycling frequency. Ultrasonic tests are performed in pulsed mode, with forced air-cooling of the specimens, and with measured and controlled specimen surface temperatures to avoid measurement artefacts caused by specimen self-heating.

2. Material and method

2.1. Material and specimen

Fatigue tests are performed with PolyEtherEtherKetone (PEEK) produced with commercially available raw material VICTREX 450G PEEK from Victrex plc. A second testing series is performed with PEEK from the same supplier reinforced with multiwall carbon nanotubes (CNT). Fillers and resin were blended via a twin screw extruder and molded via injection molding. The materials will be called PEEK and CNT reinforced PEEK in the following. Molded plaques with thickness 3.1 mm for PEEK, and 2.9 mm for CNT reinforced PEEK, respectively were produced and specimens were extracted with their length direction parallel to the flow direction. Mechanical properties of the testing material are shown in Table 1.

The specimen shapes employed in the present investigation are shown in Fig. 1. Flat samples were extracted by water jet cutting to avoid re-heating of the material. The cut edges were grinded parallel to the specimens' length direction with elastic grinding wheels (diameter 20 mm) equivalent to 1000 grit. The flat shape does not allow conventional attachment to the ultrasonic load train via a male thread. Rather, the samples were glued (with epoxy-based adhesive) to aluminum "head pieces" with a threaded portion that connects to the ultrasonic load train, and a slotted section to accept the PEEK sample. Samples must vibrate in resonance in ultrasonic testing. The resonance length for ultrasonic frequency is determined with the Finite Elements Analysis (FEA) method (linear elastic modal analysis in Autodesk Nastran InCAD). The geometries for PEEK and CNT reinforced PEEK are slightly different in overall length to account for differences in Young's modulus, mass density, and thickness, while maintaining resonance vibration at 19 kHz. The specimens feature a rectangular gauge section with a length of 4 mm and a width of 3.5 mm (after grinding).

Fig. 2 shows a comparison of stressed volumes and cyclic stress along the sample long axis for both materials, and for modal and static loading conditions, from linear elastic FEA calculations. The testing volume is considered as the material volume subjected to $\geq$ 90 % of the nominal cyclic axial stress (red in second line of Fig. 2). Ultrasonic loading yields a testing volume of 70 mm^3 for PEEK, and 68 mm^3 for CNT reinforced PEEK. For servohydraulic loading of CNT reinforced PEEK, testing volume amounts to 75 mm^3. It is apparent that the testing volumes differ by maximum 10 % which makes size effects improbable.

PEEK is a semicrystalline thermoplastic polymer. The crystallinity over the thickness of the specimen was measured by small-angle X-ray scattering (SAXS) and wide- angle X-ray diffraction (WAXD) with a RIGAKU S-max3000, including MM002 + Microfocus source (Cu-K_α, wavelength $\lambda = 0.154$ nm) and a Triton200 multiwire detector (SAXS) or a Fuji image plate system (WAXD), respectively. A 0.5 mm thin cross section perpendicular to the loading and the thickness direction was cut from the samples and measured in vacuum. Obtained 2D images were azimuthally integrated and background corrected in order to obtain the SAXS scattering curves to access the PEEK lamellar stacking arrangement and the WAXD diffractograms to access crystal structure and crystallinity.

The surface layers of both PEEK and CNT reinforced PEEK show clear orientation for both the SAXS and WAXD images. While the inner region of the CNT reinforced PEEK also shows this orientation, the inner region of the PEEK sample does not show preferred orientation. The orientation is post probably flow induced by the production process [36]. The sum of lamellar and amorphous layer thickness was evaluated according to Ref. [37] with about 14 nm stacking height. The peaks measured with

Table 1
Mechanical properties of the testing material at 23 °C; Young's modulus, yield stress $R_{p0.1}$, yield stress $R_{p0.2}$, and tensile strength from monotonic experiments at a rate of 10^{-3} s^{-1}.

Material	Density (g/cm^3)	Young's Modulus (GPa)	$R_{p0.1}$(MPa)	$R_{p0.2}$(MPa)	Tensile Strength (MPa)	Glass Transition Temperature (°C)
PEEK	1.28	3.56	53.8	64.2	98	150
CNT reinforced PEEK	1.30	4.75	66.9	74.8	102	150

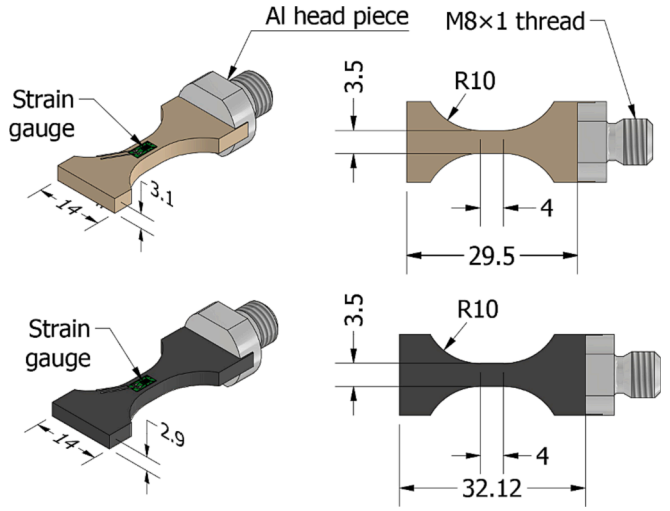

Fig. 1. Specimen geometry used in the present investigation for PEEK (top) and CNT reinforced PEEK (bottom); all dimensions in mm; specimen thickness is uniform at 3.1 mm for PEEK, and 2.9 mm for CNT reinforced PEEK, respectively; strain gauges are used for calibration.

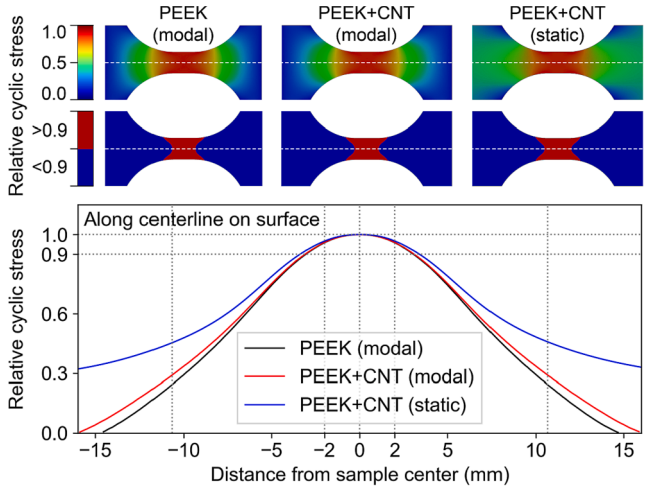

Fig. 2. FEA linear elastic modal analysis for PEEK (top panel, left column), for CNT reinforced PEEK (top panel, center column), and for a linear static analysis of CNT reinforced PEEK (top panel, right column); relative cyclic stress vs. distance from sample center for both materials, and modal and static loading conditions (bottom panel).

WAXD correspond to the spectrum reported in literature [38]. Crystallinity was evaluated with a peak deconvolution method. For the PEEK sample and the CNT reinforced PEEK sample, values of 24 % and 28 %, respectively were obtained. Despite the different orientation distribution of inner and surface areas, the crystallinity is constant over the sample cross sections.

2.2. Ultrasonic fatigue testing procedure

Fatigue tests are performed with ultrasonic fatigue testing equipment developed at the University of Natural Resources and Life Sciences, Vienna (BOKU) [2], at constant amplitude (i.e., the nominal vibration amplitude remains constant over subsequent pulses) and load ratio $R = -1$. Specimens are stimulated to resonance vibrations at a certain vibration amplitude, which is selected prior to the test. The oscillation amplitude at the ultrasonic horn, where the specimen is connected, is measured with an induction coil type vibration gauge, and is used to control cyclic loading in a closed-loop circuit. The closed-loop control ensures that the nominal vibration amplitude is reached quickly (typically within 10 ms) and without any overshoot [39]. Load cycles $\geq$ 95 % of the nominal amplitude are counted over the entire pulse duration i.e., including the build-up and decay time. Fig. 3 shows the specimen attached to the ultrasonic horn and the vibration gauge that is used to measure the movement at the ultrasonic horn. An accuracy of $\pm$ 1 % between the nominal and the measured vibration amplitude is achieved. A second closed loop control circuit guarantees that the excitation frequency of the specimen is kept at resonance frequency with an accuracy better than $\pm$ 1 Hz. The resonance frequency in the present tests was approximately 19 kHz. Resonance frequency changes over the course of a test due to crack initiation and growth, and a frequency limit is used to stop the test in case of specimen failure.

Loading of specimens is realized in pulsed mode (pulse lengths between 50 ms and 100 ms) with intermittent cooling pauses (pause lengths between 1000 ms and 4000 ms) to allow carrying off the heat generated by high frequency cycling. The high accuracy of load and

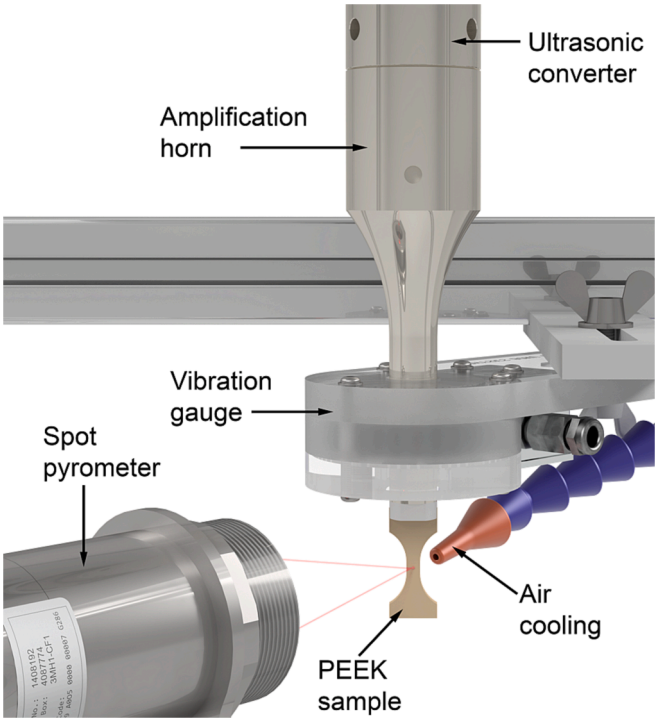

Fig. 3. Setup for ultrasonic fatigue testing of PEEK and CNT reinforced PEEK samples under fully reversed loading conditions (i.e. $R = -1$).

frequency control guarantee that the nominal vibration amplitude is reached quickly (i.e. in about 10 ms), that no overshoot occurs at the beginning of the pulse, and that the actual vibration amplitude precisely follows the nominal amplitude. Under these conditions, no influence of intermittent loading on measured lifetimes exists [39]. Additionally, compressed air cooling is used to keep specimen surface temperature below 35 °C (i.e., far below the glass transition temperature).

A spot infrared thermometer (spot ∅1 mm, <10 ms response time, sampling at a rate of 1024 s^{-1}) is used to monitor specimen temperature in every test. Fig. 4 shows a snippet of a temperature recording from a CNT reinforced PEEK specimen that was tested at the highest investigated stress amplitude of 50 MPa. Short pulses (i.e., 50 ms) and long pauses (i.e., 4000 ms) are necessary to keep specimen surface temperature below 35 °C, leading to an effective cycling frequency of 240 Hz in this experiment. Higher effective frequencies up to ~ 1.9 kHz (i.e., 100 ms pulses, 1000 ms pauses) could be used at lowest cyclic stresses.

2.3. Selection and verification of cyclic strain amplitudes in ultrasonic tests

Since loading occurs in the linear elastic regime strain amplitudes in the specimen centers and vibration amplitudes at their ends are linearly proportional. Calibration of loading with simultaneous readings from strain gauges and the vibration gauge prior to the testing series serves to determine the proportional factor between the vibration and strain amplitude. Stress amplitudes are calculated from the strain amplitudes using Hooke's law.

Samples are subjected to strain amplitudes of $\lesssim 1.5 \times 10^{-3}$ during calibration to avoid damage to the strain gauges. In the present investigation, however, ultrasonic fatigue tests are conducted at strain amplitudes of up to 10^{-2}, where strain gauges would fail immediately. Because of the large difference between calibration and testing amplitudes, it needs to be verified therefore that the very high strain amplitudes are accurately achieved.

A combination of non-contact displacement measurements and finite element analysis simulation was applied to several CNT reinforced PEEK samples that were cycled at a strain amplitude of 1.05×10^{-2} (corresponding to a stress amplitude of 50 MPa), which is the highest strain amplitude used in the present ultrasonic tests. Displacement measurements were taken at the head piece, at the upper mass section of the sample (just below the head piece), and just above the bottom edge of the sample, with a Polytec IPV–100 in–plane laser vibrometer. The proportionality between displacement amplitude at the sample's ends and strain in the center of the gauge section was derived from a linear-elastic modal simulation in Autodesk Inventor Nastran. The analysis indicates a displacement amplitude of 86.3 μm for the nominal strain amplitude of 1.05×10^{-2}. Applying the proportionality from the FEA simulation to the displacement readings from the laser vibrometer, an agreement between measured and calculated strain amplitudes within ± 2.5 % was observed.

2.4. Servohydraulic fatigue testing procedure

Conventional force-controlled fatigue tests using an Mts 810.23 servohydraulic load frame have been carried out at R = -1 and cycling frequency of 22 Hz. These experiments serve to compare fatigue lifetimes measured in ultrasonic tests to those obtained with a conventional testing method. CNT reinforced PEEK specimens have been tested with forced-air cooling in place. The specimen shape used in servohydraulic tests is the same as in ultrasonic tests. No size effect needs to be considered therefore when comparing the fatigue lifetimes measured with both techniques (as demonstrated in Fig. 2). However, the upper end of the specimen is not glued into a head piece, but both ends are directly clamped in MTS 647.10 hydraulic grips with flat MTS 641.10 Surfalloy© wedges to introduce the cyclic forces.

3. Results

3.1. S–N data

S–N data measured for unreinforced PEEK in ultrasonic fatigue tests at load ratio $R = -1$ are shown in Fig. 5. Arrows mark specimens that did not fail during 10^9 cycles or more. The stress amplitude with 50 % fracture probability for a certain number of cycles is determined according to Ref. [40] assuming a Gaussian cumulative frequency distribution of failure probabilities. With this, 50 % fracture probability at 10^9 cycles is determined at stress amplitude $\sigma_a = 21.2 \pm 4.3$ MPa.

S–N data measured for CNT reinforced PEEK at $R = -1$ are shown in Fig. 6. Data obtained in ultrasonic fatigue tests at 19 kHz cycling frequency and servohydraulic tests measured at 22 Hz are marked with different symbols and colors. Fatigue lifetimes at σ_a = 50 MPa were measured with both testing techniques. Cycles to failure are between 1.24×10^5 and 1.33×10^6 cycles in ultrasonic tests and between 3.13×10^5 and 4.68×10^6 cycles in servohydraulic tests. A two-tailed two-sample Kolmogorov-Smirnov test of log-normal lifetimes at $\sigma_a = 50$ MPa confirms the null-hypothesis of both data sets being drawn from the

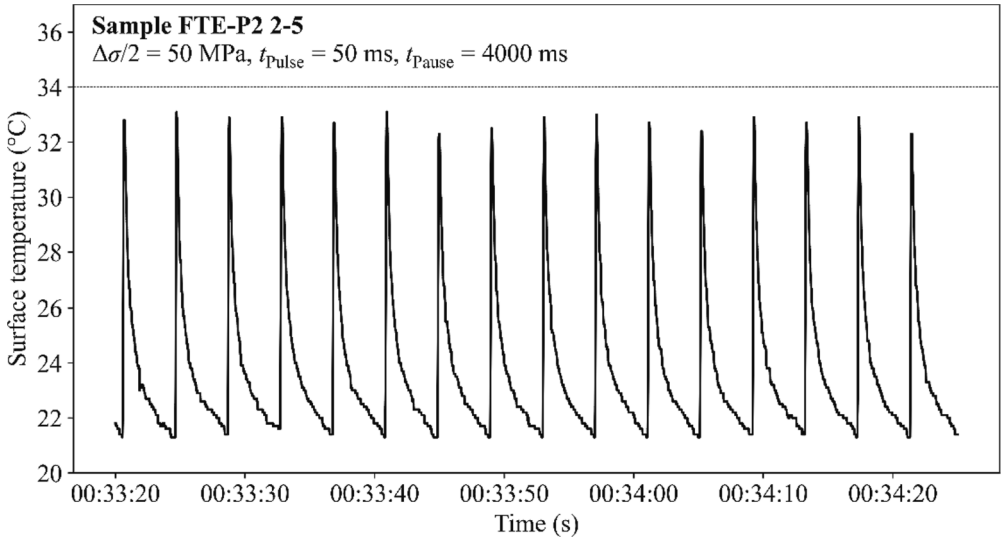

Fig. 4. Snippet of a temperature recording from a CNT reinforced PEEK sample cycled at the highest investigated stress amplitude of 50 MPa.

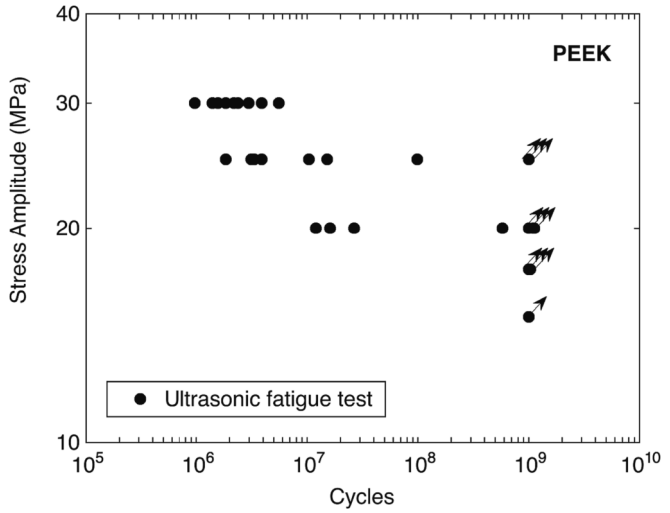

Fig. 5. *S–N* data of PEEK measured in ultrasonic fatigue tests at 19 kHz cycling frequency.

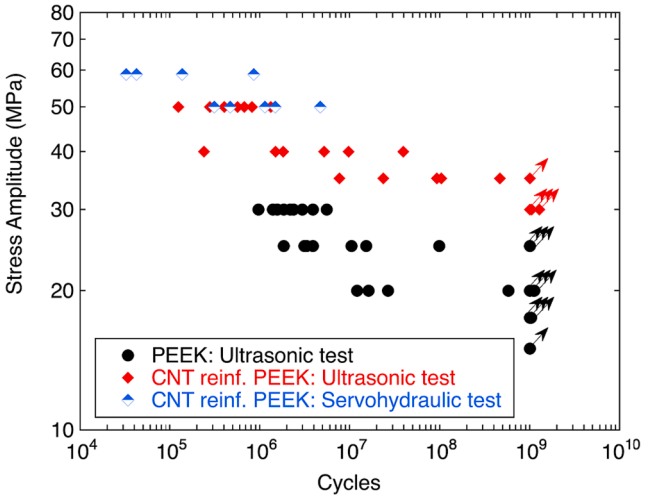

Fig. 7. *S–N* data of PEEK (black circles) and CNT reinforced PEEK measured with ultrasonic equipment (red diamonds) and servohydraulic equipment (blue diamonds).

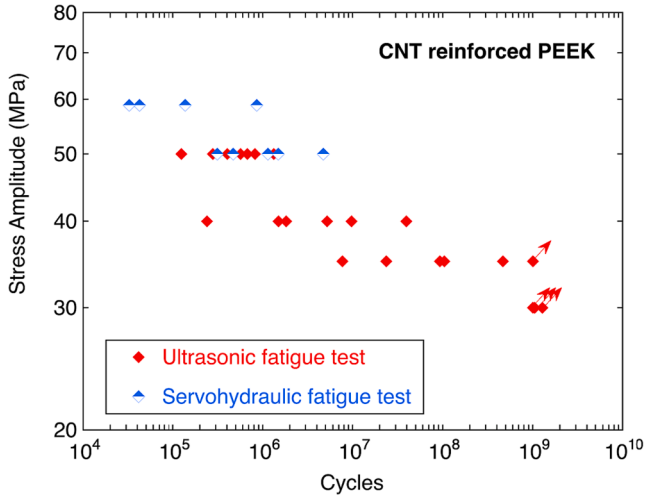

Fig. 6. *S–N* data of CNT reinforced PEEK measured in ultrasonic fatigue tests at 19 kHz cycling frequency (red symbols) and servohydraulic fatigue tests at 22 Hz (blue symbols).

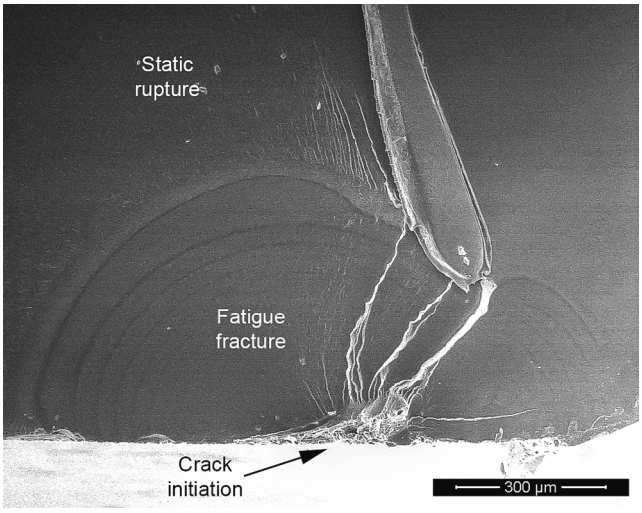

Fig. 8. Crack initiation in unreinforced PEEK, $f = 19$ kHz, $\sigma_a = 30$ MPa, $N_f = 1.6 \times 10^6$ cycles.

same underlying distribution with > 95 % confidence. Thus, no significant influence of cycling frequency on measured fatigue lifetimes can be attributed. 50 % fracture probability at 10^9 cycles for CNT reinforced PEEK is determined at stress amplitude $\sigma_a = 33.5 \pm 3.5$ MPa.

Fig. 7 shows a comparison of *S-N* data measured for PEEK and CNT reinforced PEEK. The beneficial effect of reinforcement with CNTs is obvious: All three tested CNT reinforced PEEK specimens survived 10^9 cycles at 30 MPa, whereas all eleven unreinforced specimens tested at this stress amplitude failed.

3.2. Fractography

All failed specimens were found to have failed within the 4 mm long parallel gauge section. They were examined in an optical microscope and a Field Emission Scanning Electron Microscope (FESEM) in low pressure mode. Fig. 8 shows the fracture surface of a specimen that was cycled at $f = 19$ kHz at stress amplitude 30 MPa and failed after 1.6×10^6 cycles. The fatigue crack started at the surface and produced an initially rough and structured fracture surface up to a crack depth of approximately 50 µm. Adjacent to this rough area, a flat and smooth fatigue fracture surface is visible. Striations can be observed as the only sign of plastic deformation with a spacing that presumably corresponds to crack growth during a single pulse (i.e., approx. 2000 load cycles). The fatigue crack propagated until a depth of about 0.5 mm was reached. Subsequently, the specimen failed by static rupture.

Fig. 9 shows the fracture surface of a CNT reinforced PEEK specimen that was cycled at a stress amplitude of 40 MPa. The specimen failed after 2.4×10^5 cycles, which is the lowest fatigue lifetime measured at this stress amplitude. The fatigue crack started at an internal cavity with a mean diameter of 150 µm, visible in the center of Fig. 9 (a). Stress concentration caused by this cavity leads to crack initiation, and its large size makes the short fatigue lifetime of this specimen plausible. The fatigue fracture surface appears rough and is laced with dimples. In a distance between 0.5 and 1 mm from the crack initiating cavity, the static fracture surface starts and forms a much flatter and less structured surface compared with the fatigue fracture surface. Fig. 9 (b) shows the fatigue fracture surface near the crack initiation in more detail. A heavily deformed and uneven fatigue fracture surface can be seen.

No general differences regarding morphologies and crack initiation locations were found as lifetimes transition from the HCF to the VHCF

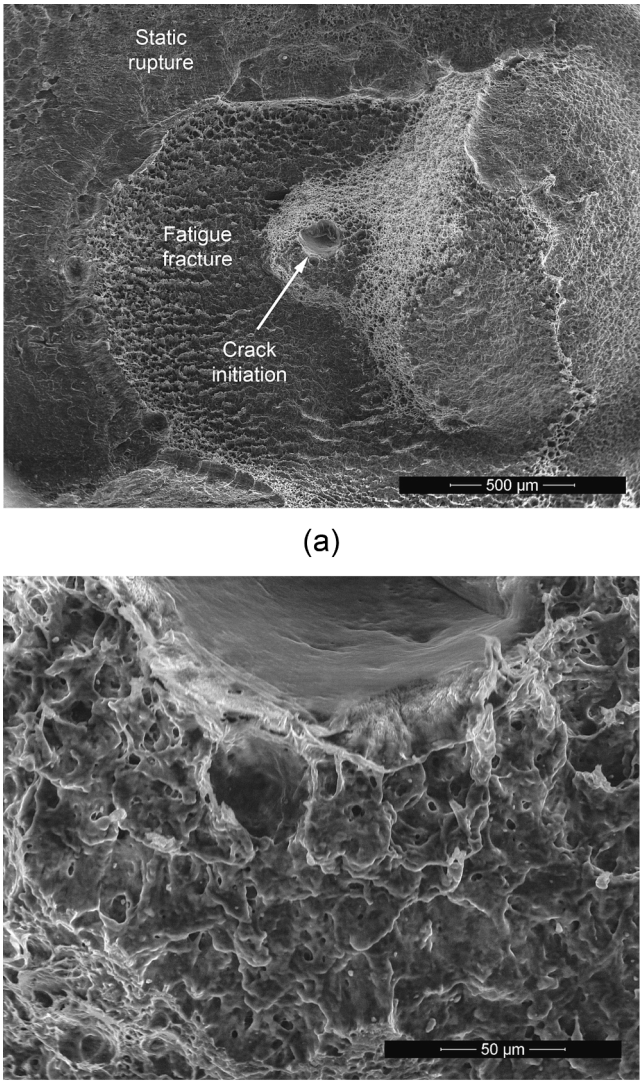

Fig. 9. Crack initiation in CNT reinforced PEEK, $f = 19$ kHz, $\sigma_a = 40$ MPa, $N_f = 2.4 \times 10^5$ cycles (a) overview of fracture surface, (b) detailed view close to crack initiating cavity.

regime, in both materials. In unreinforced PEEK specimens, the fatigue cracks started at the surface in all but one specimen. In CNT reinforced specimens, the crack started at the surface in 55 % of the specimens and in the interior in 45 %. If the crack starts in the interior, a material inhomogeneity is visible at the start of the crack, such as a void or secondary particles (suspected agglomerates of CNTs). Diameters of the crack initiating irregularities in CNT reinforced PEEK in the interior were found between 50 µm and 150 µm.

As a consequence of the fully-reversed, load controlled tests, fracture surfaces from servohydraulic tests generally hold no meaningful information, as they are heavily deformed and damaged during the very last cycles before final fracture.

4. Discussion

The ultrasonic fatigue testing method was successfully used in the present work to measure fatigue lifetimes of PEEK and CNT reinforced PEEK in the HCF and VHCF regime. CNT reinforced PEEK was additionally tested with servohydraulic equipment for verification of the ultrasonic technique. Cycling at 19 kHz and 22 Hz at the same stress amplitude delivered failures in an overlapping regime of lifetimes, which proves the validity of the ultrasonic method. Ultrasonic fatigue tests in the VHCF regime were performed in pulsed mode with 100 ms pulse and 1000 ms pause lengths which yields an effective testing frequency of 1.9 kHz. Testing times are shortened by about factor 100 compared with the servohydraulic tests, demonstrating the main benefit of ultrasonic fatigue testing.

Ultrasonic testing is different from conventional (servohydraulic) fatigue testing in several aspects. Stress amplitudes are determined by the applied force and the specimen cross section area in servohydraulic tests. Stresses cannot be directly determined in ultrasonic tests, since ultrasonic test are controlled via the vibration amplitude of the specimen's end. A correlation between vibration amplitude and strain amplitude is established prior to the test in a calibration procedure as well as by numerically calculating the linear-elastic deformation of the specimen with finite element analysis. Stress amplitudes are then calculated from strain amplitudes with the Young's modulus. During the test, the vibration amplitude, but not the strain amplitude, can be measured and controlled since strain gauges immediately fail at the high cyclic strains necessary to fatigue PEEK. It is necessary therefore, to confirm in a different way that the vibration amplitudes and consequential the strain amplitudes were actually reached. This was realized in the present work with laser optical measurements of the movement of the specimen's ends and FEA simulation of the specimen deformation.

Although no frequency effects of CNT reinforced PEEK were found in the present investigation, other studies show strain rate influences on fatigue data of (reinforced) polymers. Lower fatigue lifetimes at the higher cycling frequency are documented, if specimen temperatures increased under high frequency cycling [41–44]. Higher fatigue lifetimes at the higher cycling frequency were found, if creep played a significant role in the process of fatigue damage, which led to higher inelastic deformation at low frequency [45,46]. Accelerated fatigue crack growth at lower cycling frequencies have been measured if the contribution of creep to crack extension rates is larger for the longer duration of the load cycle [47–49]. In other investigations, frequency effects could be avoided due to intensive cooling during high frequency testing [50] or due to the limitation of loads to relatively low stress amplitudes [51].

Fatigue tests at ultrasonic as well as conventional frequency are available for glass fiber reinforced polymer (GFRP) [6,7] where frequency influences on measured lifetimes were found in one investigation [7] but not in the other [6]. These different findings may be rationalized by considering test and glass transition temperatures [52]: No frequency effect was found for the material with glass transition temperature above 130 °C [6], which is well above the specimen temperature during the test (maximum 25 °C), whereas the material with a glass transition temperature of 50 °C and tested with specimen temperature 30 °C [7] showed a frequency effect.

It is concluded in the literature [52,53] that the cycling frequency does not affect the fatigue lifetime of plastics as long as creep does not play a role and as long as the temperature is controlled and kept far below glass transition temperature. In the present ultrasonic fatigue tests, the specimens were cooled with forced air and loading was applied in pulsed mode, with pause lengths selected appropriately so that the specimen temperature remained below 35 °C. Compared with the glass transition temperature of the material (about 150 °C), the testing temperature is far lower. Stress amplitudes are less than 50 % of the static strength in ultrasonic tests. Therefore, no creep will occur, and no frequency influence on measured fatigue lifetimes is found, well in accordance with the literature [52,53].

An interesting result demonstrated for the first time with the aid of ultrasonic fatigue testing is the absence of a fatigue limit for PEEK and for CNT reinforced PEEK. In both materials, failures above 10^7 cycles and even above 10^8 cycles could be measured. Cyclic strength in the VHCF regime quantified with 50 % fracture probability at 10^9 cycles is a factor 1.57 higher for CNT reinforced than for unfilled PEEK. The effect

on the static properties is less pronounced, i.e., CNT reinforced PEEK shows a factor 1.04 higher tensile strength and a factor 1.33 higher Young's modulus than unfilled PEEK.

Fatigue fracture surfaces of CNT reinforced PEEK are rough and show dimples as a result of considerable plastic deformation at the crack tip. The fatigue fracture surfaces of unfilled PEEK are smooth and, besides striations, show no obvious signs of plastic deformation. Similar to metals, the effective rather than the nominal stress intensity factor range determines fatigue crack growth rates in PEEK [29]. Several mechanisms are active in CNT reinforced PEEK that consume energy required for crack growth and reduce the crack driving force acting at the crack tip. The respective contributions of enhanced cyclic plastic deformation, roughness induced crack closure as well as the additional energy required for fracture or pull-out of the CNTs cannot be quantified, but all these mechanisms are in total very effective to impede fatigue crack growth in CNT reinforced PEEK.

Moreover, approximately half of the CNT reinforcement PEEK specimens showed material defects with diameters between 50 μm and 150 μm (i.e., voids or secondary particles) at their crack initiation locations, whereas no obvious material inhomogeneities were found in unfilled PEEK. Still the material tested in the present condition shows strongly improved fatigue strength, which points to a good defect tolerance and supports the effectiveness of CNT reinforcement to improve the VHCF properties of PEEK.

5. Conclusions

Fatigue properties of PEEK and PEEK reinforced with multiwall CNTs have been investigated with ultrasonic and servohydraulic fatigue testing equipment. The following conclusions may be drawn.

1. Ultrasonic fatigue testing with intermitted loading with periodic cooling pauses is an appropriate technique to avoid specimen self-heating and to investigate the fatigue properties of PEEK and CNT reinforced PEEK up to the VHCF regime. Pulsed loading reduces the effective frequency in VHCF tests to the range of one Kilohertz. Still testing times can be reduced significantly compared with conventional fatigue testing methods.
2. Servohydraulic fatigue tests with CNT reinforced PEEK at a stress amplitude, where failures occurred in the HCF regime, delivered lifetimes similar to ultrasonic fatigue tests, which demonstrates the applicability of the ultrasonic method. The glass transition temperature of PEEK (about 150 °C) is much higher than the maximum specimen temperature during testing (35 °C), and creep as a possible contributor to frequency effects is therefore not active.
3. VHCF strength represented by the stress amplitude for 50 % fracture probability at 10^9 cycles is 21.2 ± 4.3 MPa for unreinforced PEEK (22 % of its tensile strength) and 33.5 ± 3.5 MPa for CNT reinforced PEEK (33 % of its tensile strength). In contrast to the fatigue properties, the static strength of CNT reinforced PEEK is only slightly (4 %) higher than that of unfilled PEEK.
4. CNT reinforcement strongly increases the plastic deformation involved in the propagation of a fatigue crack leading to a microscopically heavily deformed and rough fracture surface. Effective stress intensity factor range at the crack tip is reduced which improves the fatigue crack propagation properties and leads to good defect tolerance.

CRediT authorship contribution statement

Michael Fitzka: Conceptualization, Data curation, Formal analysis, Investigation, Methodology, Supervision, Validation, Visualization, Writing – original draft. **Bernd M. Schönbauer:** Conceptualization, Writing – review & editing. **Viktor Stojanovic:** Investigation, Methodology. **Harald Rennhofer:** Investigation, Methodology, Writing – original draft. **Helga Lichtenegger:** Conceptualization, Methodology, Resources, Writing – review & editing. **Jason W. Carroll:** Funding acquisition, Project administration, Resources. **Niloofar Sanaei:** Writing – review & editing. **Javed Mapkar:** Resources, Writing – review & editing. **Herwig Mayer:** Conceptualization, Funding acquisition, Project administration, Resources, Supervision, Visualization, Writing – original draft.

Declaration of competing interest

The authors declare that they have no known competing financial interests or personal relationships that could have appeared to influence the work reported in this paper.

Data availability

Data are subject to ongoing research and will be made public at a later time

References

[1] S. Stanzl-Tschegg, Very high cycle fatigue measuring techniques, Int. J. Fatigue 60 (2014) 2–17.
[2] H. Mayer, Recent developments in ultrasonic fatigue, Fatigue Fract. Eng. Mater. Struct. 39 (2016) 3–29.
[3] M. Fitzka, B.M. Schönbauer, R.K. Rhein, N. Sanaei, S. Zekriardehani, S.A. Tekalur, J.W. Carroll, H. Mayer, Usability of Ultrasonic Frequency Testing for Rapid Generation of High and Very High Cycle Fatigue Data, Materials 14 (2021).
[4] G.M. Domínguez Almaraz, E. Correa Gómez, J.C. Verduzco Juárez, J.L. Avila Ambriz, Crack initiation and propagation on the polymeric material ABS (Acrylonitrile Butadiene Styrene), under ultrasonic fatigue testing, Frattura Ed Integrità Strutturale 9 (2015).
[5] G.M.D. Almaraz, A.G. Martínez, R.H. Sánchez, E.C. Gómez, M.G. Tapia, J.C. V. Juárez, Ultrasonic fatigue testing on the polymeric material PMMA used in odontology applications, , Proc. Struct. Integr. 3 (2017) 562–570.
[6] D. Flore, K. Wegener, H. Mayer, U. Karr, C.C. Oetting, Investigation of the high and very high cycle fatigue behaviour of continuous fibre reinforced plastics by conventional and ultrasonic fatigue testing, Compos. Sci. Technol. 141 (2017) 130–136.
[7] C.S. Lee, H.J. Kim, A. Amanov, J.H. Choo, Y.K. Kim, I.S. Cho, Investigation on very high cycle fatigue of PA66-GF30 GFRP based on fiber orientation, Compos. Sci. Technol. 180 (2019) 94–100.
[8] Y. Shimamura, T. Hayashi, T. Fujii, K. Tohgo, Accelerated axial fatigue testing of carbon fiber reinforced plastics quasi-isotropic laminate by using ultrasonic fatigue testing machine, Fatigue Fract. Eng. Mater. Struct. 45 (2022) 2421–2424.
[9] C.-H. Jung, Y. Kang, H. Song, M.G. Lee, Y. Jeon, Ultrasonic fatigue analysis of 3D-printed carbon fiber reinforced plastic, Heliyon 8 (2022) e11671.
[10] S.A. Michel, R. Kieselbach, H.J. Martens, Fatigue strength of carbon fibre composites up to the gigacycle regime (gigacycle-composites), Int. J. Fatigue 28 (2006) 261–270.
[11] A. Hosoi, N. Sato, Y. Kusumoto, K. Fujiwara, H. Kawada, High-cycle fatigue characteristics of quasi-isotropic CFRP laminates over 108 cycles (Initiation and propagation of delamination considering interaction with transverse cracks), Int. J. Fatigue 32 (2010) 29–36.
[12] S.E. Stanzl-Tschegg, M. Papakyriacou, H.R. Mayer, J. Schijve, E.K. Tschegg, High Cycle Fatigue Crack Growth Properties of Aramid Reinforced Aluminum Laminates, in: W.W. Stinchcomb, N.E. Ashbaugh (Eds.), Composite Materials: Fatigue and Fracture, Vol. IV, ASTM, Philadelphia, 1993, pp. 637–652.
[13] M. Papakyriacou, J. Schijve, S.E. Stanzl-Tschegg, Fatigue Crack Growth Behaviour of Fiber-Metal Laminate Glare 1 and Metal Laminate 7475 with Different Blunt Notches, Fatigue Fract. Engng, Mater. Struct. 20 (1997) 1573–1584.
[14] D. Backe, F. Balle, D. Eifler, Fatigue testing of CFRP in the Very High Cycle Fatigue (VHCF) regime at ultrasonic frequencies, Composite Sci Techn 106 (2015) 93–99.
[15] D. Backe, F. Balle, Ultrasonic fatigue and microstructural characterization of carbon fiber fabric reinforced polyphenylene sulfide in the very high cycle fatigue regime, Compos. Sci. Technol. 126 (2016) 115–121.
[16] W. Cui, X. Chen, C. Chen, L. Cheng, J. Ding, H. Zhang, Very High Cycle Fatigue (VHCF) Characteristics of Carbon Fiber Reinforced Plastics (CFRP) under Ultrasonic Loading, Materials 13 (2020) 908.
[17] J. Ding, L. Cheng, Ultra-high three-point bending fatigue performance of nano-silica-reinforced CFRP, Int. J. Fatigue 145 (2021) 106085.
[18] J. Ding, L. Cheng, Ultra-high three-point bending fatigue fracture characteristics of CFRP modified by MWCNTs and fatigue life data analysis, Compos. Struct. 259 (2021) 113468.
[19] J. Li, M. Xiao, J. Ding, H. Zhu, Y. Chen, Fatigue characterization study of CFRP under hygrothermal environment based on continuum damage mechanics model, Fatigue Fract. Eng. Mater. Struct. 43 (2020) 2943–2955.
[20] J. Ding, L. Cheng, Experimental study on ultrasonic three-point bending fatigue of CFRP under ultraviolet radiation, Eng. Fract. Mech. 242 (2021) 107435.

[21] A. Premanand, F. Balle, Development of an axial loading system for fatigue testing of textile-composites at ultrasonic frequencies, Materials Letters: X 13 (2022) 100131.
[22] T. Miyakoshi, T. Atsumi, K. Kosugi, A. Hosoi, T. Tsuda, H. Kawada, Evaluation of very high cycle fatigue properties for transverse crack initiation in cross-ply carbon fiber-reinforced plastic laminates, Fatigue Fract. Eng. Mater. Struct. 45 (2022) 2403–2414.
[23] A. Premanand, F. Balle, Stress and strain calculation method for orthotropic polymer composites under axial and bending ultrasonic fatigue loads, Ultrasonics 135 (2023) 107130.
[24] B.M. Schönbauer, M. Killinger, U. Karr, M. Fitzka, U. Müller, A. Teischinger, H. Mayer, Fatigue properties of wood at different load ratios tested at 50 Hz and 20 kHz, Mater. Werkst. 53 (2022) 344–354.
[25] U. Karr, M. Fitzka, B.M. Schönbauer, T. Krenke, U. Müller, H. Mayer, Fatigue testing of wood up to one billion load cycles, Holzforschung 76 (2022) 977–984.
[26] M. Brillhart, J. Botsis, Fatigue crack growth analysis in PEEK, Int. J. Fatigue 16 (1994) 134–140.
[27] M.C. Sobieraj, J.E. Murphy, J.G. Brinkman, S.M. Kurtz, C.M. Rimnac, Notched fatigue behavior of PEEK, Biomaterials 31 (2010) 9156–9162.
[28] L. Wang, S. Shi, S. Fu, G. Chen, X. Chen, Evaluation of multiaxial fatigue life prediction criteria for PEEK, Theor. Appl. Fract. Mech. 73 (2014) 128–135.
[29] T. Colmer, S.R. Daniewicz, J.C. Newman, R. Moser, Measuring fatigue crack growth and closure in Polyether Ether Ketone (PEEK), Int. J. Fatigue 95 (2017) 243–251.
[30] R. Shrestha, J. Simsiriwong, N. Shamsaei, Mean strain effects on cyclic deformation and fatigue behavior of polyether ether ketone (PEEK), Polym. Test. 55 (2016) 69–77.
[31] R. Shrestha, J. Simsiriwong, N. Shamsaei, R.D. Moser, Cyclic deformation and fatigue behavior of polyether ether ketone (PEEK), Int. J. Fatigue 82 (2016) 411–427.
[32] K. Friedrich, R. Walter, H. Voss, J. Karger-Kocsis, Effect of short fibre reinforcement on the fatigue crack propagation and fracture of PEEK-matrix composites, Composites 17 (1986) 205–216.
[33] W.J. Evans, D.H. Isaac, K.S. Saib, The effect of short carbon fibre reinforcement on fatigue crack growth in PEEK, Composites Part A-Applied Science and Manufacturing 27 (1996) 547–554.
[34] N. Bonnheim, F. Ansari, M. Regis, P. Bracco, L. Pruitt, Effect of carbon fiber type on monotonic and fatigue properties of orthopedic grade PEEK, J. Mech. Behav. Biomed. Mater. 90 (2019) 484–492.
[35] A. Avanzini, C. Petrogalli, D. Battini, G. Donzella, Influence of micro-notches on the fatigue strength and crack propagation of unfilled and short carbon fiber reinforced PEEK, Mater. Des. 139 (2018) 447–456.
[36] J. Seo, D. Parisi, A.M. Gohn, A. Han, L. Song, Y. Liu, R.P. Schaake, A.M. Rhoades, R. H. Colby, Flow-Induced Crystallization of Poly(ether ether ketone): Universal Aspects of Specific Work Revealed by Corroborative Rheology and X-ray Scattering Studies, Macromolecules 53 (2020) 10040–10050.
[37] L. Jin, J. Ball, T. Bremner, H.-J. Sue, Crystallization behavior and morphological characterization of poly(ether ether ketone), Polymer 55 (2014) 5255–5265.
[38] S. Yu, K.P. Hariram, R. Kumar, P. Cheang, K.K. Aik, In vitro apatite formation and its growth kinetics on hydroxyapatite/polyetheretherketone biocomposites, Biomaterials 26 (2005) 2343–2352.
[39] B.M. Schönbauer, M. Fitzka, M. Jaskari, A. Järvenpää, H. Mayer, Very high cycle fatigue data acquisition using high-accuracy ultrasonic fatigue testing equipment, Mater Perform Charact 12 (2023).
[40] W.W. Maenning, Planning and evaluation of fatigue tests, in: S.R. Lampman, G. M. Davidson, F. Reidenbach, R.L. Boring, A. Hammel, S.D. Henry, W.W. Scott (Eds.), ASM Handbook Fatigue and Fracture, ASM International, Materials Park OH, 1997, pp. 303–313.
[41] J.W. Dally, L.J. Broutman, Frequency Effects on the Fatigue of Glass Reinforced Plastics, J. Compos. Mater. 1 (1967) 424–442.
[42] H.C. Kim, L.J. Ebert, Fatigue life-limiting parameters in fibreglass composites, J. Mater. Sci. 14 (1979) 2616–2624.
[43] M.R. Kharrazi, S. Sarkani, Frequency-dependent fatigue damage accumulation in fiber-reinforced plastics, J. Compos. Mater. 35 (2001) 1924–1953.
[44] V. Barron, M. Buggy, N.H. McKenna, Frequency effects on the fatigue behaviour on carbon fibre reinforced polymer laminates, J. Mater. Sci. 36 (2001) 1755–1761.
[45] G.C. Tsai, J.F. Doyle, C.T. Sun, Frequency Effects on the Fatigue Life and Damage of Graphite/Epoxy Composites, J. Compos. Mater. 21 (1987) 2–13.
[46] D. Perreux, E. Joseph, The effect of frequency on the fatigue performance of filament-wound pipes under biaxial loading: Experimental results and damage model, Compos. Sci. Technol. 57 (1997) 353–364.
[47] M.G. Wyzgoski, G.E. Novak, D.L. Simon, Fatigue fracture of nylon polymers, J. Mater. Sci. 25 (1990) 4501–4510.
[48] M. Parsons, E.V. Stepanov, A. Hiltner, E. Baer, Effect of strain rate on stepwise fatigue and creep slow crack growth in high density polyethylene, J. Mater. Sci. 35 (2000) 1857–1866.
[49] A. Pegoretti, T. Ricco, Fatigue Fracture of Neat and Short Glass Fiber Reinforced Polypropylene: Effect of Frequency and Material Orientation, J. Compos. Mater. 34 (2000) 1009–1027.
[50] R. Apinis, Accceleration of Fatigue Tests of Polymer Composite Materials by Using High-Frequency Loadings, Mech. Compos. Mater. 40 (2004) 107–118.
[51] A. Hosoi, K. Takamura, N. Sato, H. Kawada, Quantitative evaluation of fatigue damage growth in CFRP laminates that changes due to applied stress level, Int. J. Fatigue 33 (2011) 781–787.
[52] P. Shabani, F. Taheri-Behrooz, S.S. Samareh-Mousavi, M.M. Shokrieh, Very high cycle and gigacycle fatigue of fiber-reinforced composites: A review on experimental approaches and fatigue damage mechanisms, Prog. Mater Sci. 118 (2021) 100762.
[53] T.J. Adam, P. Horst, Fatigue damage and fatigue limits of a GFRP angle-ply laminate tested under very high cycle fatigue loading, Int. J. Fatigue 99 (2017) 202–214.